Towards laboratory detection of topological vortices in superfluid phases of QCD

Arpan Das, Shreyansh S. Dave, Somnath De, and Ajit M. Srivastava
Institute of Physics, Bhubaneswar 751005, India

Topological defects arise in a variety of systems, e.g. vortices in superfluid helium to cosmic strings in the early universe. There is an indirect evidence of neutron superfluid vortices from glitches in pulsars. One also expects that topological defects may arise in various high baryon density phases of quantum chromodynamics (QCD), e.g. superfluid topological vortices in the color flavor locked (CFL) phase. Though vastly different in energy/length scales, there are universal features, e.g. in the formation of all these defects. Utilizing this universality, we investigate the possibility of detecting these topological superfluid vortices in laboratory experiments, namely heavy-ion collisions. Using hydrodynamic simulations, we show that vortices can qualitatively affect the power spectrum of flow fluctuations. This can give unambiguous signal for superfluid transition resulting in vortices, allowing for check of defect formation theories in a relativistic quantum field theory system.

PACS numbers: 11.27.+d, 98.80.Cq, 25.75.-q

arXiv:1607.00480v2 [hep-ph] 26 Oct 2016

Topological defects are typically associated with symmetry breaking phase transitions. Due to their topological nature, they display various universal properties, especially in their formation mechanism and evolution. This has led to experimental studies of defect formation in a range of low energy condensed matter systems, e.g., superfluid helium, superconductors, liquid crystals etc. [2, 3] which have utilized this universality and have provided experimental checks on different aspects of the theory of cosmic defect formation, usually known as the Kibble mechanism [1]. However, it is clearly desirable to experimentally test these theories also in a relativistic quantum field theory system for a more direct correspondence with the theory of cosmic strings and other cosmic defects.

We address this possibility in this paper and focus on heavy-ion collision (HIC) experiments. One of the main aims of these experiments is to probe the QCD phase diagram which shows very rich features, especially in the regime of high baryon density and low temperatures. FAIR and NICA are upcoming facilities for HIC, dedicated to the investigation of high baryon density phases of QCD. Exotic partonic phases e.g. two flavor color superconducting (2SC) phase, crystalline color superconducting phase, color flavor locked (CFL) phase, [4] etc. are possible at very high baryon density. Transitions to these phases is associated with complex symmetry breaking patterns allowing for a very rich variety of topological defects in different phases. Even at moderately low baryon densities nucleon superfluidity (neutron superfluidity and proton superconductivity) arises. The CFL phase occurs at very high baryon densities, with baryon densities an order of magnitude higher than the nuclear saturation density (ρ_0), and temperatures up to about 50 MeV, whereas nucleonic superfluidity occurs at much lower densities, of order $(10^{-3} - 1)\rho_0$, and temperatures as low as 0.3 MeV. Interestingly, this entire vast range of densities and temperatures may be accessible at the facilities such a FAIR and NICA. As we noted above, irrespective of the energy scale, universality of defect formation allows us to infer reasonably model independent predictions about qualitative effects arising from vortex formation from these different phase transitions.

In the present day universe, superfluid phases of nucleons are expected to exist inside neutron stars [5] and resulting vortices are supposed to be responsible for the phenomenon of glitches [6]. No such observational support exists yet for the high density phases of QCD (e.g. CFL phase) in any astrophysical object. In an earlier paper, some of us have proposed the detection of such phase transitions by studying density fluctuations arising from topological defect formation and its effects on pulsar timings and gravitational wave emission [7].

All of the HIC investigations in the literature probing the high baryon density regime of QCD have focused primarily on signals related to the quark-hadron transition. We propose a somewhat different line of focus at these experiments. Some of these exotic high baryon density partonic phases also have superfluidity. For example, the CFL phase corresponds to the spontaneous symmetry breaking pattern, $SU(3)_{color} \times SU(3)_L \times SU(3)_R \times U(1)_B \rightarrow SU(3)_{color+L+R} \times Z_2$. Superfluidity arises from spontaneous breaking of $U(1)_B$ to Z_2 as the diquark order parameter for the CFL phase is not invariant under $U(1)_B$ baryon number transformations. This is also expected in somewhat lower density phases (where effects of heavier strange quark become important) such as the 2SC phase [4]. In HIC, if any of these phases arise, a superfluid transition will inevitably lead to production of superfluid vortices via the Kibble mechanism [1]. As we will discuss later, universality of defect formation in the Kibble mechanism tells that defect density of order one will be produced per correlation domain [1]. (For a second order transition, critical slowing down can affect defect formation in important ways, and is described by the Kibble-Zurek mechanism[2].)

It is immediately obvious that the most dramatic effect of presence of any vortices will be on the resulting flow pattern. We carry out detailed simulations of development of flow in the presence of vortices and study qualitative changes in the flow pattern. We will first focus on superfluid transitions in the high baryon density par-

tonic phase of QCD and later comment on the possibility of low baryon density nucleonic superfluid phase transition. We carry out hydrodynamical simulations of the evolution of a partonic system in the presence of vortices using a two-fluid picture of superfluid. We also consider a range of values for the density fraction of superfluid to normal fluid and study its effect on the signals. The two fluids are evolved, as in our earlier simulations [8], with Woods-Saxon profile of energy density with and without additional density fluctuations (though it does not appear to have crucial effects on our results). It is known that various high baryon density partonic phases (QGP, 2SC, CFL etc.) do not differ much in energy density and pressure [4]. Thus, we evolve the superfluid component with the same equation of state as the normal fluid, which is taken simply to be an ideal gas of quarks and gluons at temperature T and quark chemical potential μ_q with the energy density ϵ given as (for two light flavors) [9],

$$\epsilon = \frac{6}{\pi^2}\left(\frac{7\pi^4}{60}T^4 + \frac{\pi^2}{2}T^2\mu_q^2 + \frac{1}{4}\mu_q^4\right) + \frac{8\pi^2}{15}T^4 \qquad (1)$$

with pressure $P = \epsilon/3$. Note, as our interest is only in discussing the hydrodynamics in the partonic phase (and not in the quark-hadron transition), we do not include the bag constant. The energy-momentum tensor is taken to have the perfect fluid form,

$$T^{\mu\nu} = (\epsilon + P)u^\mu u^\nu - Pg^{\mu\nu} \qquad (2)$$

where u^μ is the fluid four-velocity. The hydrodynamical evolution is carried out using the equations, $\partial_\mu T^{\mu\nu} = 0$. Note that we do not need to use conservation equation for the baryon current as our interest is only in flow pattern requiring knowledge of ϵ and P and the ideal gas equation of state relating P and ϵ does not involve μ_q. The simulation is carried out using a 3+1 dimensional code with leapfrog algorithm of 2nd order accuracy. For various simulation details we refer to the earlier work [8]. The initial energy density profile for both fluid components (normal fluid as well as superfluid) is taken as a Woods-Saxon background of radius 3.0 fm with skin width of 0.3 fm. We take the initial central energy density ϵ_0 with temperature $T_0 = 25$ MeV and $\mu_q = 500$ MeV as representative values [4]. Initial random fluctuations are incorporated in terms of 10 randomly placed Gaussian of half-width 0.8 fm, with central amplitude taken to be $0.4\epsilon_0$.

The initial velocity profile is determined by the fluid rotation around the vortices. For the superfluid part, The magnitude of the fluid rotational velocity at distance r from the vortex center is taken as

$$v(r) = v_0\frac{r}{\xi} \quad (r \le \xi); \qquad v(r) = v_0\frac{\xi}{r} \quad (r > \xi) \qquad (3)$$

Here ξ is the coherence length. For CFL vortex, estimates in ref.[5] give $v_0 = 1/(2\mu_q\xi)$ and the coherence length is given by

$$\xi \simeq 0.26\left(\frac{100\text{MeV}}{T_c}\right)\left(1 - \frac{T}{T_c}\right)^{-1/2} \quad \text{fm.} \qquad (4)$$

We take value of superfluid transition temperature $T_c = 50$ MeV [5]. For the initial central temperature $T_0 = 25$ MeV, resulting values of $\xi = 0.7$ fm and $v_0 = 0.3$ (we take $c = 1$). (Note, even though we use 2 flavors, we use the estimates of the vortex profile for the CFL phase for order of magnitude estimates.)

The initial velocity profile for the normal fluid is determined by implementing local momentum conservation at the time of vortex formation. Vortices form here via the "Kibble mechanism" for a system which is undergoing superfluid transition via spontaneous symmetry breaking. In the two fluid picture, a part of the system undergoes the transition (fraction of particles undergoing bose condensation). It is the spatial variation of the phase of the order parameter (the superfluid gap) which leads to non-zero superfluid velocity, hence circulation for a vortex structure. This happens spontaneously everywhere once a vortex has formed during the transition (which can be a quench). The momentum balance will be achieved locally, simply by the normal component of fluid recoiling to balance the local momentum generated for the superfluid component. So, basically, some particles fall into a quantum state with non-zero momentum, which, for an isolated system, is only possible when other particles in that part of the system develop equal and opposite momentum.

The final picture is then that spontaneous generation of vortex via the Kibble mechanism leading to superfluid circulation in such a system will be accompanied by opposite circulation being generated in the normal component of the fluid. It is clear that exactly at the time of formation of the vortex, the velocity profile of the normal component will be opposite, having exactly the same form as that of the superfluid vortex. So, for the normal fluid, the initial velocity profile is taken to be exactly the same as given by Eqn.(3), but with v_0 having opposite sign, and suitably scaled for local momentum conservation depending on superfluid density fraction. This will be the correct profile if the normal fluid has very low viscosity (as it happens for QGP at RHIC energies). However, if the viscosity is large, then this velocity profile will not be sustained due to differential rotation, and will change. We have accounted for this possibility also by considering admixture of velocity profile for viscous fluid with a velocity profile $v(r) \propto r$ (even though we use non-viscous hydrodynamics). We find that this does not affect the qualitative features of our results at all, except that with large fraction of this viscous velocity profile one also gets a non-zero directed flow in the presence of vortices.

We mention that we do not simulate coupled dynamics of normal and superfluid components. Instead, we evolve the two components using separate conservation equations for the two energy momentum tensors. This allows us to simulate a delayed superfluid transition. This

models the situation when initial partonic system has too high a temperature to be in the superfluid phase, though it is still in the QGP phase, and subsequent expansion and cooling leads to crossing the phase boundary to the superfluid phase. Also, for the case of nucleon superfluidity (to be discussed below), initial high temperatures will lead to normal nucleonic phase, and only at late stages of expansion superfluid phase can arise. In a coupled fluid dynamics, this cannot be achieved as one always has a normal fluid as well as a superfluid component.

For observational signatures, we focus on the power spectrum of flow fluctuations. In a series of papers some of us have demonstrated that just like the power spectrum of CMBR, in HIC also the power spectrum of flow fluctuations has valuable information about the initial state fluctuations of the plasma [10]. We will calculate the power spectrum of flow fluctuations and study the information contained in the power spectrum about the initial vortex induced velocity fields. We focus on the central rapidity region (focusing on a thin slab of width 2 fm in z direction at z = 0) and study the angular anisotropy of the fractional fluctuation in the fluid momentum, $\delta p(\phi)/p_{av}$, where ϕ is the azimuthal angle and p_{av} is the angular average of the fluid momentum. This fluid momentum anisotropy is eventually observed as momentum anisotropy of the hadrons which are finally detected. The power spectrum of flow fluctuations is obtained by calculating the root mean square values v_n^{rms} of the n_{th} Fourier coefficient v_n of the momentum anisotropy $\delta p(\phi)/p_{av}$. We use lab fixed coordinates, so event averaged value of v_n is zero.

We use standard Kibble mechanism to estimate the probability of vortex formation. In the CFL phase, superfluidity corresponds to spontaneous breaking of U(1) symmetry (just like the case for superfluid ^{4}He). In two space dimensions, this leads to probability 1/4 for the formation of a vortex (V) or antivortex (AV) per correlation domain [1]. For the azimuthal momentum anisotropy in the central rapidity region, the relevant velocity field is essentially two-dimensional. With the correlation length of order 1 fm, and the plasma region of a radius of 3 fm, we expect number of superfluid vortices to be about 2. For definiteness, we will consider cases of 1 vortex, and a V-V pair and a V-AV pair. The locations of these are taken to be randomly distributed in the plasma region. To have clear signals, we have taken definite orientations for the vortices. We consider vortices either pointing along z axis (with random locations) or pointing along x axis (passing through the origin).

We now present results of the simulations. Fig.1 shows the effect of vortices on the flow power spectrum for a central collision at $\tau - \tau_0 = 1.68$ fm, (with $\tau_0 - 1.0$ fm). We mention that due to complexity of flow pattern, fluid evolution becomes unstable for large times, hence we show the results at relatively shorter times. However, these qualitative signals will be expected to survive even for longer times, though with possibly smaller magnitudes. As such these will apply to situations of early freezeout, e.g. for smaller nuclei, or for peripheral collisions. Fig.1 shows plots for the cases of no vortex, one vortex, a V-V pair, and a V-AV pair. In all cases, vortices are taken along the z axis with random positions. Noteworthy is a large value of the elliptic flow for the V-AV case (even though this is a central collision). For all cases with vortices we find that the elliptic flow is very large initially (see, also, Fig.2). This is clearly seen in the inset of Fig.1 for the V-AV case which also shows the dependence of elliptic flow on superfluid fraction and its time evolution. This can be detected by its effects on photon or dileption elliptic flow [14] which is sensitive to flow effects at very early stages.

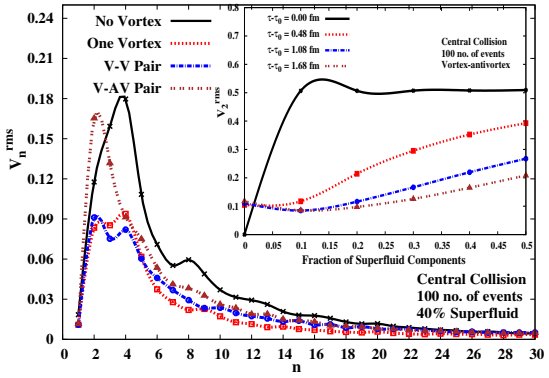

FIG. 1: Power spectrum at $\tau - \tau_0 = 1.68$ fm for central collision. Different plots show the power spectrum for the cases of no vortex, single vortex, a V-V pair, and a V-AV pair. Inset shows dependence of elliptic flow at different times on the superfluid fraction for the V-AV case showing very large initial elliptic flow.

Fig.2 shows the time evolution of the power spectrum for the case with a V-V pair (we find similar results for V-AV case as well). Note difference in the power for even and odd Fourier coefficients at earlier times. (Such a qualitatively different pattern in HIC has only been predicted in the presence of magnetic field, as reported in ref. [11]). This result also has interesting implications for the CMBR power spectrum. It is known that low l modes of CMBR power spectrum also show difference in even-odd modes [12]. It is possible that this feature may be indicative of the presence of a magnetic field, or presence of some vorticity during the very early stages of the inflation.

Fig.3 presents the case of non-central collisions. Here we consider an ellipsoidal shape for the plasma region as appropriate for a non-central collision with semi-minor axis along the x-axis, and initial spatial eccentricity = 0.6. Here we plot v_2 for a single event (not the rms value), for two cases, a V-AV pair pointing in z direction and located on the x-axis at $x = \pm 1.5 fm$ respectively, and the other case with a single vortex lying along the x-axis. Both cases show strongly negative elliptic flow at initial stages. Fig.4 also shows large (negative) values of v_4 for both these cases which arises from vortex induced elliptic flow being in the orthogonal direction to

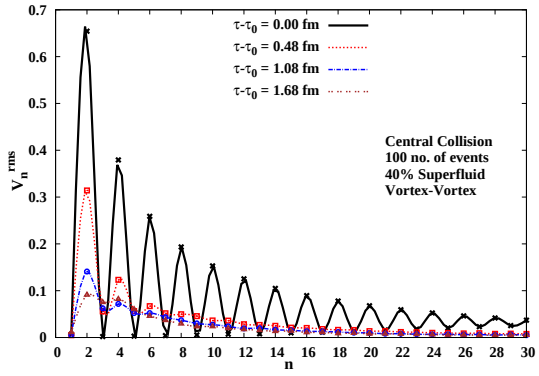

FIG. 2: Time evolution of the power spectrum for the case with a V-V pair showing the difference in the power for even and odd Fourier coefficients for early times.

the shape induced elliptic flow. These large values of negative elliptic flow as well as v_4 may be observed if the freezeout occurs at early times (in smaller systems, or in peripheral collisions) and should also leave imprints on other observables such as on v_2 for photons [14]. Note that negative elliptic flow can arise in relatively low energy HIC due to squeeze-out effects [15]. However, for low energy collisions (as we discuss below for nucleonic superfluidity), a vortex induced negative elliptic flow is completely uncorrelated to the elliptic shape of the event (which can be inferred from independent observables), hence can be distinguished from the squeeze-out effect. Further , at higher energies (where CFL phase may be expect to arise), no squeeze-out is expected, so a negative elliptic flow can signal vortex formation. We have also carried out all the simulations with a delay of up to 1 fm in the onset of superfluid transition (following our modeling of the two fluid picture as explained above). The results remain essentially unchanged with various plots showing changes of order only few percent.

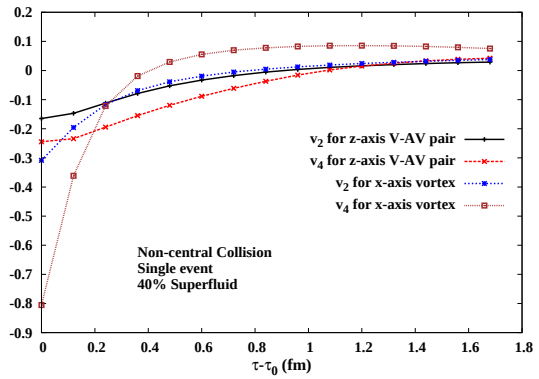

FIG. 3: Plot of v_2 and v_4 for non-central collisions for a V-AV pair along z axis, and a single vortex along the x axis, showing negative elliptic flow at initial stages as well as large (negative) values of v_4.

We now discuss the possibility of detecting nucleonic superfluidity in HIC. Though neutron superfluid condensate is expected to exist inside several nuclei, these systems are too small to demonstrate bulk superfluid phase and its associated superfluid vortices, as are expected inside a neutron star. Calculations for neutron stars show that nucleonic superfluidity is expected in range of densities from $10^{-3}\rho_0$ (for $^1S_0$ pairing of neutrons) to few times ρ_0 (for $^3P_2 -^3 F_2$ pairing). The critical temperature can range from 0.2 MeV to 5 MeV (depending on the nuclear potential used [16]). Temperatures and densities of this order are easily reached in HIC at relatively low energies. For example, at the FOPI-facility at GSI Darmstadt, temperatures of about 17 MeV (with $\rho \sim 0.4\rho_0$) were reported in Au-Au collisions at 150 MeV/nucleon lab energy [17]. Temperatures of order 4-5 MeV were reported in Au-Au collisions at E/A = 50 MeV, at heavy-ion synchrotron SIS [18]. Thus temperatures/densities appropriate for the transition to the nucleonic superfluid phase can easily be reached in HIC. Universality of defect formation implies that the qualitative aspects of our results in this paper (for the CFL phase) will continue to hold even in this lower density regime. FAIR and NICA are ideal facilities for probing even this low energy regime with detectors suitable for measurements with which flow power spectrum analysis can be performed. Detection of signals as discussed in this paper can provide a clean detection of nucleonic superfluid vortices. It is worth emphasizing the importance of focused experiments for creating a nucleonic system of several fm size which can accommodate nucleonic superfluid vortices. Direct experimental evidence of these vortices and controlled studies of their properties can provide a firm basis for our understanding of neutron stars. This is all the more important in view of the fact that gravitational waves from rotating neutron stars and their collisions will be thoroughly probed by LIGO and upcoming gravitational wave detectors.

We conclude by pointing out that the signals we have discussed show qualitatively new features in flow anisotropies signaling the presence of vortices and the underlying superfluid phase in the evolving plasma. These qualitative features are expected to be almost model independent, solely arising from the vortex velocity fields. We mention that one has to properly account for the effects due to jets, resonance decays etc. to properly account for genuine hydrodynamic flow fluctuations. We hope to address these issues in a future work. Also, we have not included error bars in our plots to avoid overcrowding of the plots. The number of events was chosen suitably large (100 events) so that the main qualitative features of the plot are above any statistical fluctuations. (Our focus is mainly on the qualitative patterns of the plots, in the spirit of the universal features of topological vortices forming at varying energy scales, and not on precise numerical value.) Similar signals are expected from nucleonic superfluid vortices which can arise in low energy HIC providing direct experimental access to the physics of pulsars. Detection of these vortices will allow

probing Kibble mechanism for these relativistic quantum field theory systems, providing a more direct correspondence with the theory of cosmic defects. For second order transitions, one will also be able to use the Kibble-Zurek mechanism to probe the effects of critical slowing down and gain knowledge of various critical exponents for the specific transition.

We are very grateful to Rajeev Bhalerao, Partha Bagchi, Srikumar Sengupta, Biswanath Layek, and Pranati Rath for useful discussions.

[1] T.W.B. Kibble, J. Phys. **A 9**, 1387 (1976).
[2] W.H. Zurek, Phys. Rep. **276**, 177 (1996).
[3] See, for example, special section on condensed matter analogues of cosmology, J. Phys. **G 25** (2013).
[4] M.G. Alford, A. Schmitt, K. Rajagopal, and T. Schafer, Rev. Mod. Phys. **80**, 1455 (2008).
[5] K. Iida and G. Baym, Phys. Rev. **D 66**, 014015 (2002).
[6] J.M. Lattimer and M. Prakash, Astrophys. J. **550**, 426 (2001).
[7] P. Bagchi, A. Das, B. Layek, and A.M. Srivastava, Phys. Lett. **B 747**, 120 (2015); arXiv: 1412.4279.
[8] Saumia P.S. and A.M. Srivastava, arXiv: 1512.02136.
[9] J. Cleymans, R.V. Gavai, and E. Suhonen, Phys. Rep. **130**, 217 (1986).
[10] A. P. Mishra, R. K. Mohapatra, P. S. Saumia, and A. M. Srivastava, Phys. Rev. **C 77**, 064902 (2008); Phys. Rev. **C 81**, 034903 (2010).
[11] A.M. Srivastava, Talk presented in the conference *QCD Chirality Workshop 2015* at Physics Dept. UCLA, Jan. 2015.
[12] P. K. Aluri and P. Jain, Mon. Not. Roy. Astron. Soc. **419**, 3378 (2012).
[13] P.F. Kolb, J. Sollfrank, and U. Heinz, Phys. Rev. **C 62**, 054909 (2000).
[14] R. Chatterjee and D. K. Srivastava, Nucl.Phys. **A 830**, 503C (2009).
[15] A. Andronic, FOPI Collaboration, Phys. Lett. **B 612**, 173 (2005).
[16] L. Amundsen and E.Ostgaard, Nucl. Phys. **A 442**, 163 (1985), *ibid*, **A 437**, 487 (1985).
[17] W. Reisdorf, et al., Nucl. Phys. **A 612**, 493 (1997).
[18] V. Serfling et al., Phys. Rev. Lett. **80**, 3928 (1998).